

Characterization of a Novel Hybrid Anti-corrosive System Comprising Graphene Nano Platelets and Non-Metal-containing Anti-corrosive Pigments

William Weaver
Applied Graphene Materials UK Ltd.
Wilton Centre
Redcar, Cleveland, TS10 4RF
UK

Lynn Chikosha
Applied Graphene Materials UK Ltd.
Wilton Centre
Redcar, Cleveland, TS10 4RF
UK

Gaven Johnson
Applied Graphene Materials UK Ltd.
Wilton Centre
Redcar, Cleveland, TS10 4RF
UK

Matthew Sharp
Applied Graphene Materials UK Ltd.
Wilton Centre
Redcar, Cleveland, TS10 4RF
UK

ABSTRACT

Applied Graphene Materials UK Ltd.^{†1} produces a number of graphene nano-platelet (GNPs) dispersions, enabling properties such as electrical/thermal conductivity, mechanical properties, gas permeability and barrier type to be achieved.

Anti-corrosive pigments have come under environmental pressure. The challenge is to develop anti-corrosive systems with performance equal to that of current anti-corrosive pigments. Prior work has demonstrated that very small additions of GNPs decreased water vapor transmission rates and extended time to initial corrosion and has been explained by the tortuous pathway created by the addition of GNPs to a host matrix. It has also been postulated that there is an anodic/cathodic process taking place in conjunction with typical active anti-corrosive pigments.

This work is benchmarking GNPs against and in combination with commercially available anti-corrosive pigments via electrochemical, corrosion, and mechanical testing. We seek to characterize the mechanisms by which GNPs work as anti-corrosive pigments and investigate synergistic effects which will allow improvements in coatings anti-corrosive performance. Electrochemical AC impedance Spectroscopy (EIS) and corrosion potential (OCP) measurements has been used to probe the properties of GNP-epoxy coatings. In their simplest form, values of impedance provide useful information concerning the passive barrier properties of a coating.

Key words: Graphene, Nano-platelets, Corrosion, Epoxy, Anti-Corrosive, Potentiostatic

^{†1} Tradename

INTRODUCTION

Coatings are widely used to protect metals from corrosive environments, therefore understanding their long term breakdown and the mechanisms of protection, either active or passive are key to the development of long term performance. Protective coatings have essentially three mechanisms; electrochemical, physiochemical as well as being a function of adhesion. The electrochemical behavior of coatings containing active anti-corrosion pigments such as Zinc Phosphate is well understood in the context of a macroscopic defect such as a scribe introduced during cyclic or continuous salt spray testing. It is typical for the coating technologist to combine mechanisms to achieve the optimum performance of a coating. To be able to combine these individual mechanisms it is important to understand their relationship and the correlation of permeability with anticorrosive protection¹. Organic coatings are not impermeable to water and an understanding of the behavior of intact coatings has been extensively studied. The current model relies on the formation of hydrophilic pathways through the coating, forming multiple microscopic defects enabling access of water and salts to the metal surface. Nguyen² proposed that these pathways are a result of hydrolysis and consequent leaching of unreacted materials. Epoxy based systems which constitute a major part of today's primer technology are however highly resistant to hydrolysis and the formation of hydrophilic pathways is considered to be a result of the localized water uptake and leaching.

Water uptake in epoxy based coatings has been widely studied using various techniques NMR^{3,4}, FTIR^{5,6} and dielectric spectroscopy^{7,8}. Epoxies are known to be hygroscopic with water absorption demonstrating Fickian diffusion kinetics. Various studies have shown that the apparent equilibrium water content correlates initially to the polarity of the polymer network and secondly to the available free volume^{9,10,11,12}. Soles et al¹⁰, have proposed a model in which water uptake is dominated by transport through the free volume providing access for polar sites permitting hydrogen bonding, hydroplasticisation and steady growth of hydrophilic pathways. Morsch et al¹³ confirmed Soles proposed mechanism using FTIR. Additional studies^{14,15} have demonstrated a slower non Fickian water uptake. This is thought to be caused by hydroplasticisation and swelling of the network allowing slow water sorption. It is expected that Fickian behavior and uptake into the available free volume dominates over short time periods with non Fickian behavior dominating long term character of the films. Morsch et al¹⁶ confirmed such a model using FTIR and AFM demonstrating rapid uptake into free volume and interaction with hydrogen bonding sites adjacent to micro voids which causes hydroplasticisation and disruption of the polymer network.

Graphene in various chemical and physical forms has been studied to determine whether the material operates by a mechanism, which is based on a passive (barrier) mechanism or also combines an active electrochemical mechanism. It has been reported that graphene based coatings offers excellent short term barrier protection^{17,18,19}, although once such graphene coatings have been breached, graphene may actually act to electrochemically promote corrosion at the metal interface. The work carried out here will evaluate the performance of graphene nanoplatelet modified primers. Two grades of graphene nano-platelets (Grade 10 – reduced graphene oxide, Grade 35 – graphene) are utilized, which are differentiated by surface area and morphology in a C3 (ISO 12944)²⁰ type epoxy primer and contrasted with typical systems containing commercially available anti-corrosive pigments.

A specific attempt in this work was made to explore the use of “Green” non-metallic anti-corrosive pigments (calcium oxide-modified silica) in an effort to eliminate the use of Zinc Phosphate based materials which while non-hazardous to humans are a marine pollutant.

EXPERIMENTAL PROCEDURE

Material and Sample Preparation

The Graphene Nanoplatelets used are characterized in Figure 1. Dispersions of graphene nanoplatelets (GNPs) were manufactured at concentrations of 1% (grade 35) and 5% (grade 10). They were manufactured using a wetting stage within a centrifugal mixer, then passed through a three roll mill in order to ensure a complete dispersion and consistent particle size.

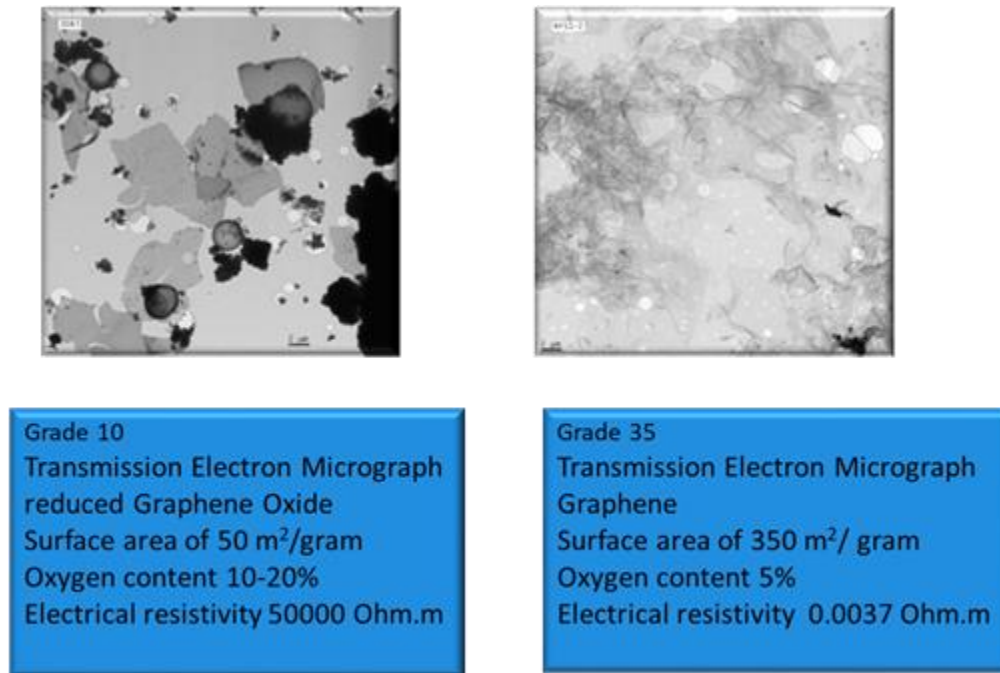


Figure 1: GNP grades utilized in coating formulation

A basic epoxy coating was formulated using the materials listed below, on a standard laboratory overhead stirrer: Xylene, Butanol, Epoxy Resin, Barium Sulphate, Urea-Amino Resin, Carbon Black, Graphene Nano-platelet dispersions, zinc phosphate, calcium oxide-modified silica. The coating formulation and manufacturing process used is detailed in Table 1. Table 2 Sets out the formulation variants assessed. Epoxy paint was cured with polyamine hardener to give a stoichiometry of 85%.

Coatings were applied to mild steel panels measuring 150mm x 100mm x 2mm (5.9in x 3.9in x 0.08in). Panel preparation was by Grit blasting to SA2-1/2, using irregularly shaped chrome/nickel steel shot followed by degreasing with acetone. Coating application was by a conventional spray gun using a 1.2mm (0.05in) tip to a dry film thickness of 60-75 microns (3mil) +/-20 microns (0.7mil). The panels were prepared in duplicate for each of the tests to be carried out. The panels were placed in a corrosion chamber, running ASTM G85 annex 5 (prohesion)²¹ for a period of up to 5000 hours. Duplicate panels were prepared for assessment at intervals of 500, 1000, 2000, 3000, and 5000 hours, meaning that 10 in total were assessed during the test. The panels were assessed for creep from scribe, blistering, and general appearance using methods: ISO4628-3 Corrosion²², ISO4628-2 creep²³ and ISO4628-8 blistering²⁴.

Table 1
Primer formulation and Manufacturing Process

Item	RM Name	Weight %
<i>Charge items 1, 2, 3, 4 and 5, mix at high speed (2000rpm) for 10 minutes</i>		
1	Epoxy	14.78
2	Amino Resin	0.28
3	Dispersant	0.46
4	Xylene	5.62
5	Bentonite thixotrope	0.42
<i>Check Gel is homogenous and free of bits. Continue mixing if not</i>		
<i>Add items 6 to10. Mix at high speed (2000rpm) for 15 minutes. Check grind <25microns</i>		
6	Butanol	2.28
7	Xylene	5.62
8	Titanium Dioxide	12.60
9	(Anticorrosive pigment)	4-8 (Variable)
10	Blanc Fixe	50.11
<i>Add items 12 (GNP formulation) or 13. Mix at medium speed (1000rpm) for 15 minutes</i>		
12	(GNP Dispersion)	0-10 (Variable)
13	Epoxy	9.27
14	Xylene	0

Table 2
Formulation variations evaluated

Coating	GNP Content
Standard	None
Standard + 8% Zn ₃ (PO ₄) ₂	None
Standard + 4% Zn ₃ (PO ₄) ₂	None
Standard calcium oxide-modified silica	None
Standard	Grade 10 at 0.5%
Standard + 8% Zn ₃ (PO ₄) ₂	Grade 10 at 0.5%
Standard + 4% Zn ₃ (PO ₄) ₂	Grade 10 at 0.5%
Standard + calcium oxide-modified silica	Grade 10 at 0.5%
Standard	Grade 35 at 0.1%
Standard + 8% Zn ₃ (PO ₄) ₂	Grade 35 at 0.1%
Standard + 4% Zn ₃ (PO ₄) ₂	Grade 35 at 0.1%
Standard calcium oxide-modified silica	Grade 35 at 0.1%

Mechanical Testing

Each of the coated samples were subjected to basic mechanical tests including: Taber Abrasion, Conical Mandrel (Elongation ASTM D522²⁵), Impact, and Adhesion. Abrasion resistance was carried out using a Taber Abrasion machine, running cycles of 2500 revolutions with abrasive wheels. Each sample was weighed using a precision balance, and the mass loss after each test was calculated. Impact testing was carried out using a 1kg weight dropped from a height of 1m, and assessed for cracking using method: ASTM D2794 - 93(2004)²⁶. Adhesion was carried out by fixing stainless steel adhesion dollies to the coating sample using a two-component epoxy adhesive. Samples were cured for a period of 7 days, the dollies were removed using a precision adhesion tester giving a measurement of the force required to remove in Mega Pascals (MPa), and an indication of the mechanism of coating failure whether it be adhesive or cohesive.

Water vapor transmission

Water vapor transmission through the prototype coating with and without GNP's were carried out according to Test Method ASTM D 1653-03 using Test Method B²⁷, with Grade 10 tested at 1% and Grade 35 at 0.1% loading by weight.

Over coating interval/adhesion

Adhesion testing was carried out using a sharp blade to create a cross hatch. Following a seven day period of curing at ambient temperature, the coatings were assessed and rated on a scale of 0-5 (Table 3). At each test interval the coatings were re-assessed when wet, looking at the intercoat adhesion and the adhesion to the substrate. Following a period of 24 hours, the adhesion was re-assessed to determine recovery

Table 3
Rating classification for intercoat adhesion testing

Rating	Intercoat Adhesion	Adhesion to Substrate
5	No separation	No detachment
4	Little to no separation	Force required to cause detachment
3	Force required to separate coatings	Minor detachment from cut area
2	Minimal force required to separate coatings	Significant detachment from cut area
1	Coatings separate easily	Coating scheme is easily removed
0	Coatings separate without cut	Delamination before test

Electrochemical Testing

Panels of each coating were prepared for electrochemical testing on a Gamry^{†2} Interface 1010E potentiostat and ECM8 Multiplexer. The multiplexer permitted the sequential testing of 8 channels.

AC impedance (EIS) and open circuit potential (OCP) were taken at approximately 3 hour intervals for each sample over the course of 1 week. Measurements were made by attaching a Gamry^{†2} PCT1 paint test cell containing a counter electrode, a saturated calomel reference electrode, and a conductive electrolyte solution of 5 wt.% NaCl to the coated panels. All tests cells were housed collectively in a custom built Faraday cage to reduce the risk of external interferences.

^{†2} Trade name

For AC impedance studies, the main portion of the measurements were carried out using Gamry's^{†2} propriety software. An AC voltage of 20 mV was applied, with a zero DC bias over a frequency range of 1 MHz to 50 mHz, with ten measurements for every decade in the studied frequency range. Equivalent circuits data fitting was performed using Gamry's Echem Analyst software.

Open Circuit Potential (OCP) measurements of the metal substrate were measured against a saturated calomel electrode (SCE). Prior to the commencement of testing, each of the electrodes were cleaned and replaced as over time and continuous electrochemical testing, reference electrodes may no longer provide an accurate potential value, or may have an unacceptably large impedance value.

Panels were prepared by application of coatings to Impress^{†3} CR4 grit blasted mild steel panels measuring 150mm x 100mm x 2mm. They were applied by a conventional spray gun using a 1.2mm tip to a dry film thickness of 100 microns (4mil) +/-20 microns. Panels were tested intact and scribed to the metal (scribe length 25mm (0.98in, scribe width 0.1mm (0.004in)). Scribed panels provided direct access of the 5wt% NaCl solution to the metal. It was anticipated that exposure of the metal in this fashion would enable observation of an ongoing electrochemical effect due to the incorporation of the graphene in the prototype primer or synergistic electrochemical activity when used in conjunction with an anti-corrosive pigment.

RESULTS

Prohesion testing (ASTMG85 annex 5)^{†1}

After 1000 hours, the majority of panels were showing signs of corrosion to varying degrees. Samples with 4% $Zn_3(PO_4)_2$ with Grade 10, as well as Grades 10 with both Pigments A and B continued to perform very well with limited signs of corrosion, and minimal scribe creep. The coating with no GNPs or active pigmentation had corroded beyond recognition. After 5000 hours exposure Grade 10 with 4% $Zn_3(PO_4)_2$ and Pigment A continue to show little to no corrosion. Critically systems containing Grade 10 combined with Pigment A or reduced $Zn_3(PO_4)_2$ appear to offer significantly reduced creep from the scribe, low level of blistering and corrosion, up to 5000 hours All Salt Spray results for Creep, Blistering and Corrosion were rated on scales, taken from ISO4628-2, 3, and 8 ^{22,23,24}

Table 4
1000 hrs Cyclic Salt Spray ASTM G85 annex 5 (prohesion) results

Paint	Primary Anti-corrosive	GNP	Creep (mm)	Blistering Quantity	Size (ISO)	Corrosion	Comments
1	None	None	>10	0	S0	Ri5	Very poor
2	None	Grade 10 at 0.5%	>10	0	S4	Ri5	Corroded across whole face
3	None	Grade 35 at 0.1%	3	0	S0	Ri3	Corrosion spotting across face
4	8% $Zn_3(PO_4)_2$	None	4	1	S3	Ri5	Corrosion across face
5	8% $Zn_3(PO_4)_2$	Grade 10 at 0.5%	2	0	S0	Ri1	Corrosion spotting across face
6	8% $Zn_3(PO_4)_2$	Grade 35 at 0.1%	2	0	S0	Ri2	Corrosion spotting across face
7	4% $Zn_3(PO_4)_2$	None	8	1	S3	Ri5	Corrosion across face
8	4% $Zn_3(PO_4)_2$	Grade 10 at 0.5%	4	0	S0	Ri0	Good
9	4% $Zn_3(PO_4)_2$	Grade 35 at 0.1%	>10	0	S0	Ri5	Completely corroded
10	4% $Zn_3(PO_4)_2$	None	>10	2	S4	Ri5	Completely corroded
11	4% $Zn_3(PO_4)_2$	Grade 10 at 0.5%	2	0	S0	Ri1	Corrosion spotting across face
12	4% $Zn_3(PO_4)_2$	Grade 35 at 0.1%	>10	0	S0	Ri5	Very poor
13	Pigment A	None	3	0	S0	Ri3	Corrosion spots starting
14	Pigment A	Grade 10 at 0.5%	1	0	S0	Ri2	Good
15	Pigment A	Grade 35 at 0.1%	>10	3	S4	Ri5	Corroded across whole face

^{†3} Trade name

Table 5
5000 Hours Cyclic Salt Spray ASTM G85 annex 5 (prohesion) results

Paint	Primary Anti-corrosive	GNP	Creep (mm)	Blistering Quantity	Size (ISO)	Corrosion	Comments
1	None	None	>10	0	S0	Ri5	Very poor
2	None	Grade 10 at 0.5%	>10	0	S4	Ri5	Corroded across whole face
3	None	Grade 35 at 0.1%	>10	0	S0	Ri5	Corrosion spotting across face
4	8% Zn ₃ (PO ₄) ₂	None	>10	1	S3	Ri5	Corrosion across face
5	8% Zn ₃ (PO ₄) ₂	Grade 10 at 0.5%	>10	0	S0	Ri5	Corrosion spotting across face
6	8% Zn ₃ (PO ₄) ₂	Grade 35 at 0.1%	>10	0	S0	Ri5	Corrosion spotting across face
7	4% Zn ₃ (PO ₄) ₂	None	>10	1	S3	Ri5	Corrosion across face
8	4% Zn ₃ (PO ₄) ₂	Grade 10 at 0.5%	5	1	S2	Ri2	Corrosion spreading from scribe
9	4% Zn ₃ (PO ₄) ₂	Grade 35 at 0.1%	>10	0	S0	Ri5	Completely corroded
10	4% Zn ₃ (PO ₄) ₂	None	>10	2	S4	Ri5	Completely corroded
11	4% Zn ₃ (PO ₄) ₂	Grade 10 at 0.5%	>10	0	S0	Ri5	Corrosion spotting across face
12	4% Zn ₃ (PO ₄) ₂	Grade 35 at 0.1%	>10	0	S0	Ri5	Very poor
13	Pigment A	None	>10	0	S0	Ri5	Corrosion spots starting
14	Pigment A	Grade 10 at 0.5%	1	0	S0	Ri2	Good
15	Pigment A	Grade 35 at 0.1%	>10	3	S4	Ri5	Corroded across whole face

Mechanical Test Results

Incorporation of GNP's into the coatings does not appear to materially impact the mechanical performance of the prototype primer in a positive or negative manner (Tables 6-9). It is not possible to identify any significant influence on behavior, however further study/optimization of the prototype should enable a primer to be developed with comparable properties to those commercially available..

Table 6
Conical Mandrel Test Results

		Cracking (mm)	Elongation (%)
1	None	0	<35
2	None	120	3
3	None	12	19
4	8% Zn ₃ (PO ₄) ₂	4	21
5	8% Zn ₃ (PO ₄) ₂	4	21
6	8% Zn ₃ (PO ₄) ₂	4	21
7	4% Zn ₃ (PO ₄) ₂	4	21
8	4% Zn ₃ (PO ₄) ₂	6	23
9	4% Zn ₃ (PO ₄) ₂	100	5
10	4% Zn ₃ (PO ₄) ₂	0	<35
11	4% Zn ₃ (PO ₄) ₂	0	<35
12	4% Zn ₃ (PO ₄) ₂	0	<35
13	Pigment A	120	3
14	Pigment A	120	3
15	Pigment A	11	19

Table 7
Adhesion Test Results

Paint	Primary Anti-corrosive	GNP	Force (mPa)			Comment
			Rating 1	Rating 2	Average	
1	None	None	2	2.25	2.13	50% Adhesive failure
2	None	Grade 10 at 0.5%	3	3.5	3.25	100% Cohesive failure
3	None	Grade 35 at 0.1%	1.5	2	1.75	100% Cohesive failure
4	8% Zn ₃ (PO ₄) ₂	None	2	2	2.00	50% Adhesive failure
5	8% Zn ₃ (PO ₄) ₂	Grade 10 at 0.5%	1	1	1.00	100% Cohesive failure
6	8% Zn ₃ (PO ₄) ₂	Grade 35 at 0.1%	2	0.8	1.40	100% Cohesive failure
7	4% Zn ₃ (PO ₄) ₂	None	1.25	1.25	1.25	50% Adhesive failure
8	4% Zn ₃ (PO ₄) ₂	Grade 10 at 0.5%	1.5	1.9	1.70	5% Adhesive, 95% cohesive failure
9	4% Zn ₃ (PO ₄) ₂	Grade 35 at 0.1%	1.75	2	1.88	70% Adhesive, 30% cohesive failure
10	4% Zn ₃ (PO ₄) ₂	None	2.8	2.8	2.80	20% Adhesive, 80% cohesive failure
11	4% Zn ₃ (PO ₄) ₂	Grade 10 at 0.5%	1.5	1.8	1.65	Glue failure
12	4% Zn ₃ (PO ₄) ₂	Grade 35 at 0.1%	2.25	2.8	2.53	100% Cohesive failure

Table 8
Taber Abrasion test Results

Paint	Primary Anti-corrosive	GNP	100 cycles, 1 Kg weight, CS-10 discs			
			Initial Mass (g)	Final Mass (g)	Mass loss (mg)	Wear Rating
1	None	None	67.9412	67.9023	38.9	389
2	None	Grade 10 at 0.5%	67.4874	67.4414	46	460
3	None	Grade 35 at 0.1%	66.4083	66.3544	53.9	539
4	8% Zn ₃ (PO ₄) ₂	None	66.8564	66.8217	34.7	347
5	8% Zn ₃ (PO ₄) ₂	Grade 10 at 0.5%	67.3164	67.2630	53.4	534
6	8% Zn ₃ (PO ₄) ₂	Grade 35 at 0.1%	67.0665	67.0396	26.9	269
7	4% Zn ₃ (PO ₄) ₂	None	68.1364	68.1008	35.6	356
8	4% Zn ₃ (PO ₄) ₂	Grade 10 at 0.5%	67.2025	67.1745	28	280
9	4% Zn ₃ (PO ₄) ₂	Grade 35 at 0.1%	67.6039	67.5674	36.5	365
10	4% Zn ₃ (PO ₄) ₂	None	68.0394	68.0097	29.7	297
11	4% Zn ₃ (PO ₄) ₂	Grade 10 at 0.5%	67.3551	67.3154	39.7	397
12	4% Zn ₃ (PO ₄) ₂	Grade 35 at 0.1%	67.1761	67.1399	36.2	362

Table 9
Impact Results

Paint	Primary Anti-corrosive	GNP	Cracking begins: Height (cm) 1Kg Weight									
			10	20	30	40	50	60	70	80	90	100
1	None	None	X	X								
2	None	Grade 10 at 0.5%	X									
3	None	Grade 35 at 0.1%	X									
4	8% Zn ₃ (PO ₄) ₂	None		X								
5	8% Zn ₃ (PO ₄) ₂	Grade 10 at 0.5%					X					
6	8% Zn ₃ (PO ₄) ₂	Grade 35 at 0.1%	X									
7	4% Zn ₃ (PO ₄) ₂	None	X									
8	4% Zn ₃ (PO ₄) ₂	Grade 10 at 0.5%							X			
9	4% Zn ₃ (PO ₄) ₂	Grade 35 at 0.1%			X							
10	4% Zn ₃ (PO ₄) ₂	None	X									
11	4% Zn ₃ (PO ₄) ₂	Grade 10 at 0.5%	X									
12	4% Zn ₃ (PO ₄) ₂	Grade 35 at 0.1%	X									

Water Vapor Transmission

Water vapor transmission of the prototype primer with grade 10 gave the lowest WVTR (i.e. best barrier properties) with 30% reduction in water vapor transmission while grade 35 gave a 22% reduction in in WVTR (Figure 2).

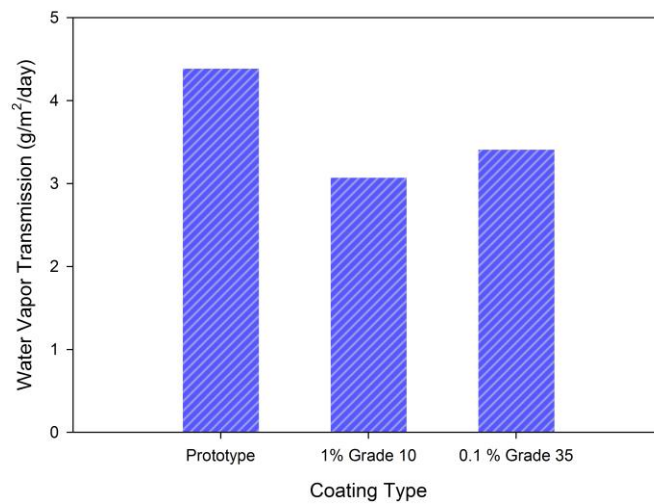


Figure 2: Water Vapor Transmission

Overcoating Interval/Adhesion

Application of a solvent based topcoat over the prototype and the GNP modified prototype primers using extended overcoating intervals shows no demonstrable reduction in intercoat adhesion when wet or on recovery (Table 10).

Table 10
Over coating interval/adhesion Results

1st Coat	2nd Coat	Overcoating Interval	Initial	Initial	Wet		Recovery	
			Intercoat Adhesion	Substrate Adhesion	Intercoat Adhesion	Substrate Adhesion	Intercoat Adhesion	Substrate Adhesion
Prototype	Topcoat	1 day	4	5	4	5	5	4
Prototype	Topcoat	3 day	4	5	4	5	5	4
Prototype	Topcoat	7 day	4	5	5	4	4	4
Prototype + Grade35	Topcoat	1 day	4	5	4	5	5	4
Prototype + Grade35	Topcoat	3 day	4	5	4	5	5	4
Prototype + Grade10	Topcoat	1 day	5	5	5	4	5	4
Prototype + Grade10	Topcoat	3 day	5	5	5	4	4	4
Prototype + Grade10	Topcoat	7 day	5	5	4	5	4	4

Potentiostatic and Electrochemical Testing

The Impedance of the unscribed films, shown in Figure 3, demonstrates the clear barrier performance of Grade 10 in conjunction with pigment A and $Zn_3(PO_4)_2$. Grade 35 while providing an improved impedance is not as effective as grade 10 reflecting the water vapor transmission results. Interestingly both pigments A and $Zn_3(PO_4)_2$ offer the lowest impedance of the modified prototype systems Grade A showing a continual decline over the time period tested potentially reflecting a greater degree of solubility and activity. Impedance of the scribed films, shown in Figure 4, shows continued performance and barrier effect of the films containing GNP's. $Zn_3(PO_4)_2$ shows little difference from the prototype while pigment A demonstrates a higher level of impedance. A significant result is the synergistic behavior of Grade 10 with Pigment A which continues to show significant performance in contrast to grade 35 or $Zn_3(PO_4)_2$ /Grade 10 formulation.

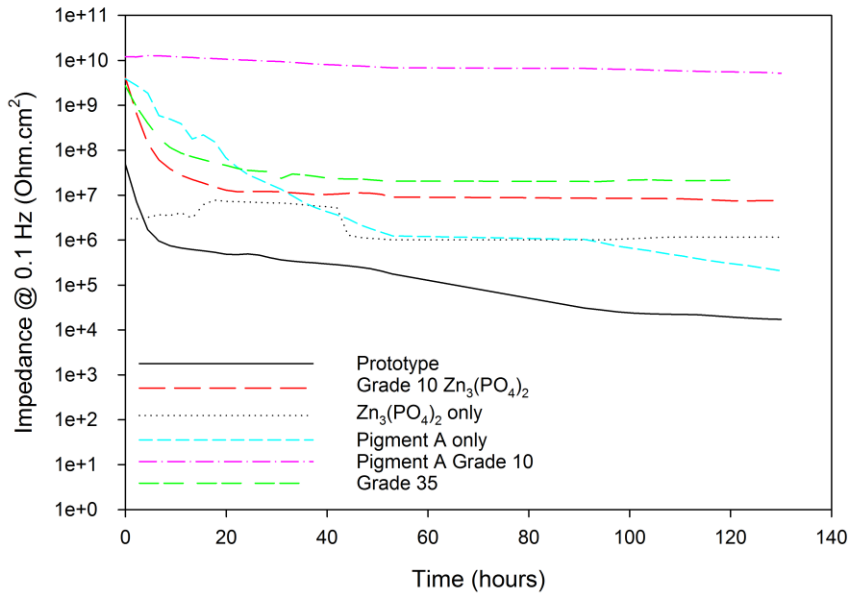


Figure 3: Impedance of unscribed coatings

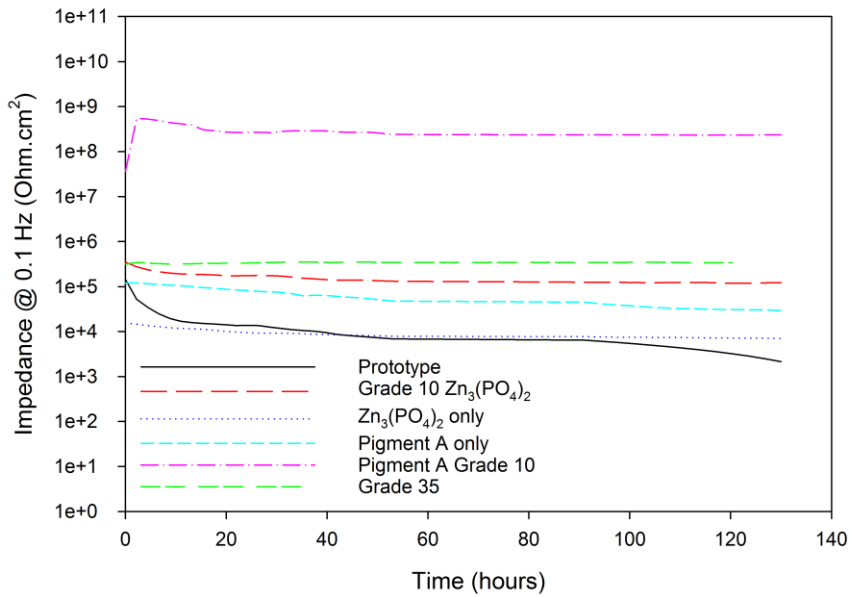


Figure 4: Impedance of scribed coatings

Figure 5 shows the OCPs of unscribed films in addition to the recorded OCP values for steel. The prototype shows a steady fall as expected with both Pigment A and $Zn_3(PO_4)_2$ modified films showing a raised OCP compared to the prototype over the timescale of the measurement. Pigment A shows a sharper decline in potential compared to $Zn_3(PO_4)_2$ again potentially reflecting solubility and activity. GNP modified films show lower OCP potentials initially than the prototype. Grade 35 is stable and eventually achieves a potential equivalent to the prototype. The Grade 10 modified film modified with Pigment A demonstrates an initial rise in potential partially reflecting the decrease seen in Pigment A itself. Grade A with $Zn_3(PO_4)_2$ demonstrates a steady potential which eventually becomes equivalent to the prototype. Scribing of the films significantly reduces the OCP potential of the GNP modified films in general (Figure 6). There is a marked difference in the behavior of the $Zn_3(PO_4)_2$ and Pigment A modified films. Pigment A alone shows a significant reduction in OCP potential when scribed compared

to $Zn_3(PO_4)_2$, interestingly when Pigment A is combined with Grade 10 although initial OCP potential is very low it increases with time whereas grade 10 when combined with $ZnPO_4$ behaves more typically of $Zn_3(PO_4)_2$ modified films alone. Grade 35 appears to suggest initial cathodic behavior but stabilizes to offer an OCP potential slightly below the prototype.

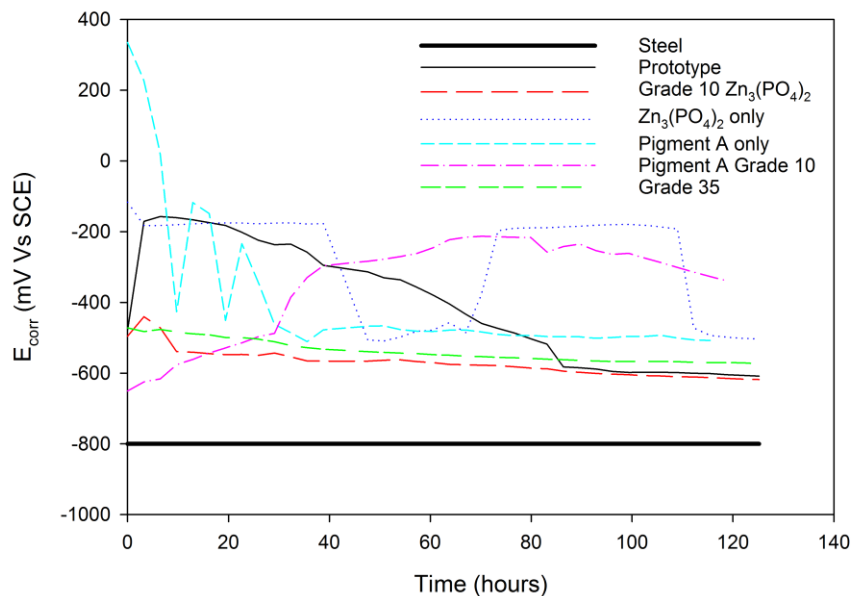


Figure 5: OCP of unscribed coatings

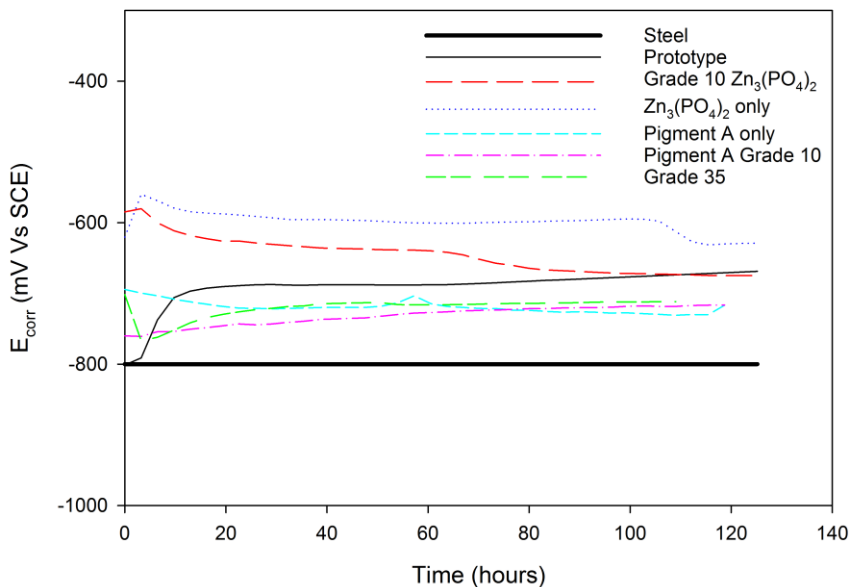


Figure 6: OCP of scribed coatings

Discussion

A traditional epoxy primer contains an active inhibitor such as zinc phosphate. Zinc phosphate is slightly soluble in water and partially dissociates into zinc ions and phosphate (PO_4^{3-}). PO_4^{3-} may then react with Fe^{2+} (available via damage to the film such as that formed by a scribe) from the anode reaction to form iron phosphate –and form a passivation layer at the metal surface- thus blocking the anode reaction. In contrast, when studying a pure barrier material (i.e. not electrochemically active), then we would expect to see corrosion at the scribe on an immersed panel. The use of a pure barrier coating does not remove the potential for the metal surface to corrode: any breaches of 'electrochemically neutral' coatings would result in corrosion at the point of breach.

Graphene has been proposed to be a multifunctional additive having both electrochemical and physicochemical properties. The behavior of graphene is highly dependent on the form and functionality. In this work we are using graphene nanoplatelets of reduced graphene oxide (Grade 10) and graphene (Grade 35). The reduced graphene oxide has a high electrical resistance (50,000 Ohm.m) while the graphene GNP (grade 35) exhibits conductive behaviour (electrical resistance 0.0037Ohm.m). Nevertheless both systems are carbon and could cause galvanic corrosion. That this is not seen and that there is no apparent electrochemical effect on the scribed samples is ascribed to the encapsulation of the platelets in non-conducting resin and their level of use being below the reported percolation threshold for this grade (28). The GNP's when incorporated into the primer on their own improve the barrier properties as shown by the impedance measurements. It is only however when Grade 10 is combined with active pigments that we see clear synergistic behaviour. As expected the OCP measurements of Grade 10 based systems suggest that the synergistic performance when combined with anti-corrosive pigment is influenced by the nature of the pigment and it's apparent solubility. Grade 35, exhibits poorer impedance and no evidence of continuous electrochemical contribution to the corrosion resistance. This suggests that the primary mechanism of the GNP grades is physiochemical by extending the diffusional pathway creating the so called tortuous path. Accepting the models proposed to date for water absorption of undamaged films, it is anticipated that the number of hydrophilic pathways is unlikely to increase on introduction of GNP's as an additive if the film Pigment Volume Concentration remains the same. It is possible therefore that the synergistic behavior of Grade 10 with Zinc Phosphate and Pigment A is due to a difference in the morphology of the GNP's and their interaction with the host resin. The net effect is however a physicochemical barrier effect to water which may result in a higher degree of localized hydroplasticisation and a steeper decrease in water concentration through the film. The net effect of such a mechanism may be the preservation of the active pigment for a longer period resulting in enhanced salt spray resistance; this would however be a function of both the physiochemical impact of the graphene and graphene morphology, together with the solubility and passivation rate of the individual pigments. Additional studies are required to fully determine the exact mechanism of the enhanced performance, which is observed in the salt spray resistance.

The mechanical properties of the films showed no consistent increase or decrease in performance, however there was no major failure of the properties measured, so it is difficult to determine if the graphene nano-platelets had any significant influence in the performance of the coating. It is likely that the other pigmentation within the system (barytes, titanium dioxide) are more influential on the mechanical properties than the graphene nano-platelets.

CONCLUSIONS

The addition of GNP in the forms used have been demonstrated to be capable of providing enhanced corrosion resistance as tested using cyclic salt spray resistance. It is apparent that the degree of enhanced corrosion performance is dependent on the nature of the GNP morphology, functionality and interaction with the host resin at one level and specific interaction with the anti-corrosive pigment at another. The exact detail of the mechanism leading to the observed performance improvement is

unclear at this time but would suggest a complex physiochemical impact by the GNP influencing the electrochemical behaviour of the pigment. It has however been possible in this work to demonstrate that a primer may be formulated with non-metal based pigments with significant corrosion performance.

REFERENCES

1. F.L Floyd, R.G Groseclose, C.M Frey, Mechanistic model for corrosion protection via paint, *J Oil Col Chem Assoc*, 66, 11, 1983, 329 – 341
2. T.Nguyen, J.B.Hubbard, J..M Pommersheim, Unified model for the degradation of organic coatings on steel in a neutral electrolyte *J. Coat Technol.*, 68, 855, 1996, 45-56
3. J. Zhou, J.P.Lucas, *Polymer*, Hygrothermal effects of epoxy resin . Part I : the nature of water in epoxy, 40, 1999, 5505-5512
4. S. Luo, J. Leisen, C.P. Wong, Study on mobility of water and polymer chain in epoxy and its influence on adhesion *J Appl. Polymer Sci*, 85, 2002, 1-8
5. S. Cotugno, G Mensitieri, P.Musto, L Sanguigno, Molecular Interactions in and Transport Properties of Densely Cross-Linked Networks: A Time-Resolved FT-IR Spectroscopy Investigation of the Epoxy/H₂O System, *Macromolecules*, 38, 3, 2005 801-811
6. J. Mijovic, H. Zhang, Local Dynamics and Molecular Origin of Polymer Network–Water Interactions as Studied by Broadband Dielectric Relaxation Spectroscopy, FTIR, and Molecular Simulations, *Macromolecules*, 36, 4, 2003, 1279-1288
7. I.D.Maxwell, R.A.Pethrick, Dielectric studies of water in epoxy resins *J.Appl.Polym.Sci* ,28, 7, 1983, 2363-2379
8. C.Grave, I.McEwan, R.A.Pethrick, *J.Appl.Polym.Sci* , Influence of stoichiometric ratio on water absorption in epoxy resins. 69, 1998, 2369-2376
9. L.Li, Y.Yu, Q.Wu, G.Zhan, S.Li *Corros Sci* , Effect of chemical structure on the water sorption of amine-cured epoxy resins, 51,2009, 3000-30006
10. C.L. Soles, A.F.Yee, *J.Polym.Sci.Part B: Polym. Phys*, A Discussion of the Molecular Mechanisms of Moisture Transport in Epoxy Resins, 38 ,2000, 792-802
11. M.Jackson, M Kausik, S Nazaenko, S.Ward, R. Maskell, J Wiggins, *Polymer*, Effect of free volume hole-size on fluid ingress of glassy epoxy networks, 52, 2011, 4528-4535
12. M.T.Aronhime, X.Peng, J.K.Gillham, R.D.Small, *J.Appl.Polym.Sci*, Effect of time-temperature path of cure on the water absorption of high T_g epoxy resins, 32,1986, 3589-3626
13. S.Morsch, S.Lyon, P.Greensmith,S.D.Smith, S.R.Gibbon, *Prg.Org.Coat*, Water transport in an epoxy–phenolic coating78, 2015, 293-299
14. Y.C.Lin, X.Chen, *Polymer*, Moisture sorption–desorption–resorption characteristics and its effect on the mechanical behavior of the epoxy system, 46, 2005 ,11994-12003
15. C.Wu, W.Wu, *Polymer* Atomistic simulation study of absorbed water influence on structure and properties of crosslinked epoxy resin 48, 2007, 5440-5448
16. S.Morsch, S.Lyon, P.Greensmith, S.R Gibbon *Faraday Discuss*, Mapping water uptake in organic coatings using AFM-IR 180, 2015, 527-542
17. Schriver, W.Regan, W.J. Gannett, A.M.Zanieweski, M.F. Crommie, A.Zettl, *ACS Nano* Graphene as a Long-Term Metal Oxidation Barrier: Worse than Nothing 7,7,5763-5768,2013
18. A.U.Chaudry, V Mittal, B Mishra, *RSC Adv* Inhibition and promotion of electrochemical reactions by graphene in organic coatings 5,80635-80368,2015
19. L. Kyhl, S.F. Nielsen, A.Grubišić Čabo, A.Cassidy, J. A. Miwab, L. Hornekær *Faraday Discuss* Graphene as an anti-corrosion coating layer, 180,495,2015
20. ISO 12944-5 :2018 Paints and varnishes - Corrosion protection of steel structures by protective paint systems
21. ASTM G85 annex 5 (prohesion) Dilute Electrolyte Cyclic Fog/Dry Test.
22. ISO4628-3:2016 Paints and varnishes – Evaluation of degradation of coatings – Designation of quantity and size of defects, and of intensity of uniform changes in appearance – Part 3: Assessment of degree of rusting

23. ISO4628-2:2016 Paints and varnishes -- Evaluation of degradation of coatings -- Designation of quantity and size of defects, and of intensity of uniform changes in appearance -- Part 2: Assessment of degree of blistering
24. ISO4628-8:2012 Paints and varnishes -- Evaluation of degradation of coatings -- Designation of quantity and size of defects, and of intensity of uniform changes in appearance -- Part 2: Assessment of degree of blistering
25. Elongation ASTM D522 Standard Test Methods for Mandrel Bend Test of Attached Organic Coatings
26. ASTM D2794 - 93(2004) Standard Test Method for Resistance of Organic Coatings to the Effects of Rapid Deformation (Impact).
27. ASTM D 1653-03 Standard Test Methods for Water Vapor Transmission of Organic Coating Films
28. Applied Graphene Materials, Technical Application note, Conductivity 2018